Journal of Materials Chemistry C

Accepted Manuscript

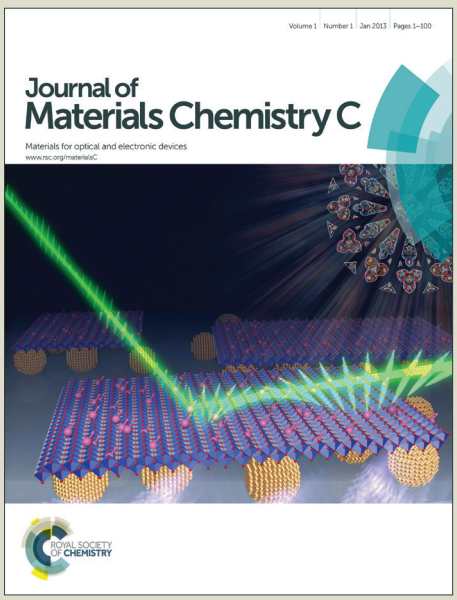

ROYAL SOCIETY OF CHEMISTRY

www.rsc.org/materialsC

Journal Name

RSCPublishing

ARTICLE

Novel 1,8-naphthalimide derivatives for standard-red organic light-emitting device applications

Cite this: DOI: 10.1039/x0xx00000x

Shuai Luo,[‡a] Jie Lin,[‡b] Jie Zhou,[a] Yi Wang,[a] Xingyuan Liu,*[b] Yan Huang,[a] Zhiyun Lu,*[a] and Changwei Hu*[a]

Received 00th January 2012,
Accepted 00th January 2012

DOI: 10.1039/x0xx00000x

www.rsc.org/

Three red-emissive D-π-A-structured fluorophores with aromatic amine as donor, ethene-1,2-diyl as π-bridge, and 1,8-naphthalimide as acceptor subunits, namely (*E*)-6-(4-(dimethylamino)styryl)-2-hexyl-1*H*-benzo[*de*]isoquinoline-1,3(2*H*)-dione (**Nap1**), (*E*)-2-(2,6-di(isopropyl)phenyl)-6-(4-(dimethylamino)styryl) -1*H*-benzo[*de*]isoquinoline-1,3(2*H*)-dione (**Nap2**) and (*E*)-2-(2,6-di(isopropyl)phenyl)-6-(2-(1,1,7,7-tetramethyl-2,3,6,7-tetrahydro-1*H*,5*H*-pyrido[3,2,1-*ij*]quinolin-9-yl)vinyl)-1*H*-benzo[*de*]isoquinoline-1,3(2*H*)-dione (**Nap3**), were designed and synthesized. In-depth investigations on the correlations between their molecular structures and photophysical characteristics revealed that the presence of an electron-rich 4-dimethylaminophenyl donor moiety in compound **Nap1** could endow it with red emission (e.g., λ_{PLmax} = 641 nm in the host/guest blend film with 14 wt% guest composition); the replacement of the *n*-hexyl group of **Nap1** bonding to the imide nitrogen atom into a more bulky 2,6-di(isopropyl)phenyl one would result in compound **Nap2** with more alleviated concentration quenching; while the alteration of the 4-(dimethylamino)phenyl donor subunit of **Nap2** into a more electron-donating 1,1,7,7-tetramethyljulolidin-9-yl substituent would render compound **Nap3** with more improved chromaticity (e.g., λ_{PLmax} = 663 nm in 14 wt% guest-doped film). Consequently, **Nap3** could not only emit standard-red fluorescence with satisfactory chromaticity, but also show suppressed intermolecular interactions. Using **Nap3** as the dopant, a heavily-doped standard-red organic light-emitting diode (OLED) with device configuration of ITO/MoO_3 (1 nm)/TcTa (40 nm)/**CzPhONI**:**Nap3** (14 wt%) (20 nm)/TPBI (45 nm)/LiF (1nm)/Al (80 nm) was fabricated, and the Commission Internationale de L'Eclairage coordinates, maximum external quantum efficiency and maximum current efficiency of this OLED are (0.67, 0.32), 1.8% and 0.7 cd A^{-1}, respectively. All these preliminary results indicated that 1,8-naphthalimide derivatives could act as quite promising standard-red light-emitting materials for OLED applications.

1. Instruction

Owing to their merits like solid-state self-emission, wide viewing angle, facile color tunability and processability, organic light-emitting devices (OLEDs) have been considered as quite competitive candidates for flat-panel display applications.[1] In comparison with phosphorescent OLEDs, fluorescent ones are more suitable with respect to display applications due to their faster response as well as lower efficiency roll-off.[2] For full-color display applications, it is necessary to develop red, green, and blue fluorescent OLEDs with high efficiency and appropriate chromaticity, yet compared with that of blue[3a] and green[3b] devices, the performance of red fluorescent OLEDs with good chromaticity is unsatisfactory. For example, although the current efficiency (*CE*) of red OLEDs with Commission Internationale de L'Eclairage (CIE) coordinates of (0.63, 0.37) could reach 11.5 cd A^{-1},[4] their chromaticity is far from standard-red whose CIE coordinates should be close to (0.67, 0.33) according to the stipulation from the National Television Standards Committee. As far as standard-red OLEDs are concerned, although according to a technical report from Idemitsu Kosan Co., high performance devices with *CE* of 11.0 cd A^{-1} could be achieved,[5] no detailed information about the molecular structures of the emitting materials and the device structures could be found; while in scientific literature reports, the performance of standard-red OLEDs was rather poor, with their maximum *CE*s lower than 3.0 cd A^{-1}, and external quantum efficiencies (*EQE*s) less than 4.0%.[6] In addition, due to the notorious concentration quenching of the guest fluorophores, the best standard-red OLED bearing guest/host doping structure (CE_{max}: 1.6 cd A^{-1}) has just a low doping-level of 2 wt%,[6d] hence the manufacturing process should be precisely controlled to acquire good device reproducibility.[7] Consequently, it is highly demanded to exploit novel high performance standard-red fluorophores with suppressed concentration quenching,[6c,8] so that OLEDs with relatively high doping-levels or even self-hosted device structure could be achieved.

Generally, red electrofluorescent materials could be classified into two main categories, namely compounds bearing polycyclic

aromatic hydrocarbon (PAHs) structures and compounds showing intramolecular charge-transfer (ICT) character with D-π-A

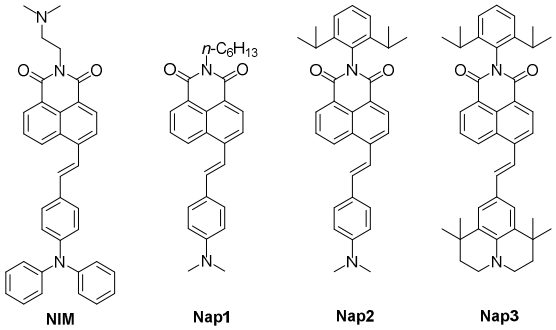

Figure 1 Molecular structures of **NIM**, **Nap1**, **Nap2** and **Nap3**.

molecular structures (where D denotes electron-donor and A denotes electron-acceptor).[8-10] To acquire standard-red fluorescence, PAHs compounds should possess relatively large conjugation systems, e.g., polyacenes[11a] and porphyrins[11b,c]. Yet to prepare these compounds, delicate synthetic and purifying procedures have to be involved.[12] Additionally, serious concentration quenching is often observed in these PAHs due to their intense intermolecular interactions.[10] On the other hand, ICT-featured red fluorophores bearing D-π-A molecular skeletons have attracted much attention due to their more facile molecular tailoring.[13] Currently, the reported red electrofluorescent ICT-compounds could be assorted, according to their acceptor constructive units, as maleimide derivatives,[14] benzothiadiazole derivatives,[15] fumaronitrile derivatives,[6f,16] and 4-dicyanomethylene-4*H*-pyran derivatives[17] etc. However, despite the fact that 1,8-naphthalimide is a widely-used acceptor subunit for constructing high performance green[18] and yellow[19] ICT-featured electroluminescent (EL) materials, quite limited success has been achieved in terms of high performance orange and red ones. In 2003, using 1,8-naphthalimide and quinoxaline as the acceptor segments, Lee *et al*.[20] reported an naphthalimide luminogen, but the OLED based on it could only emit orange-red EL with λ_{ELmax} of 608 nm. Subsequently, Tian *et al*.[21] reported that D-A fluorophores with 1,8-naphthalimide as the acceptor subunit could act as red EL materials, yet both the chromaticity and the performance of the OLED are unsatisfactory (λ_{ELmax} = 620 nm, L_{max} (maximum brightness) is 15 cd m^{-2}). Although in 2005, Cheng *et al*.[22] have fabricated red OLEDs with CIE coordinates of (0.63, 0.36) using 1,8-naphthalic anhydride derivatives as light-emitting materials, the CE_{max} of these devices is as low as 0.6 cd A^{-1}. Nevertheless, our recent work has revealed that 1,8-naphthalimide derivative could act as high performance orange EL guest material, and the corresponding OLED shows CE_{max} of 7.2 cd A^{-1}, EQE_{max} of 3.6%, and L_{max} of 16800 cd m^{-2}.[23] Despite the fact that the CIE coordinates of this device are just (0.56, 0.44), its high performance has triggered our speculation that through rational molecular design, 1,8-naphthalimide derivatives may also act as quite promising standard-red EL materials.

Recently, it has been reported that the D-π-A-structured 1,8-naphthalimide derivative **NIM** (structure shown in Figure 1) could emit intense orange fluorescence in solid state (λ_{PLmax} = 597 nm).[24] To construct fluorophores with more red-shifted photoluminescence (PL) emission bands than that of **NIM**, herein, we altered the 4-(diphenylamino)phenyl (DPAP) donor segment of **NIM** into a more electron-rich 4-(dimethylamino)phenyl (DMAP) or 1,1,7,7-tetramethyljulolidin-9-yl (TMJ) donor segment, and constructed three objective compounds (**Nap1**~**3**, structures shown in Figure 1). Additionally, to alleviate the intermolecular interactions, a bulky 2,6-di(isopropyl)phenyl substituent was bonded to the imide nitrogen atom of **Nap2** and **Nap3**. As expected, **Nap1**~**3** all could emit standard-red fluorescence in thin solid film state, and **Nap2** and **Nap3** show more suppressed concentration quenching than **Nap1**. Using **Nap3** as the guest dopant, a high performance standard-red OLED with a relatively heavy doping-level of 14 wt% was achieved. The device shows CIE coordinates of (0.67, 0.32), EQE_{max} of 1.8%, and CE_{max} of 0.7 cd A^{-1}, indicating that 1,8-naphthalimide derivatives should be promising candidates as high performance standard-red EL materials.

2. Experimental section

2.1 General information

All the reagents involved in the synthetic procedures were commercially available and used without purification unless otherwise stated. Cyclohexane (CHX), tetrachloromethane, toluene (Tol), chloroform, tetrahydrofuran (THF), dichloromethane (DCM), acetone, *N,N*-dimethyl formamide (DMF) were of analytical grade and were distilled freshly prior to use. ^{1}H NMR and ^{13}C NMR spectra were recorded on a BRUKER AVANCE AV II-400 MHz spectrometer in DMSO-d_6 or $CDCl_3$ using TMS as the internal standard. High resolution MS spectra were recorded on a Shimadzu LCMS-IT-TOF. FT-IR spectra were recorded on a Perkin-Elmer 2000 infrared spectrometer with KBr pellets under ambient atmosphere. UV-Vis absorption spectra were measured on a Perkin-Elmer Lambda 950 scanning spectrophotometer. PL spectra were recorded on a Perkin-Elmer LS55 fluorescence spectrophotometer at 298 K. The absolute PL quantum yields (QYs) of both solution and film samples were determined on a FluoroMax-4 spectrofluorometer (Horiba Jobin Yvon) equipped with an integrating sphere and digital photometer. Both the two fluorimeters have been corrected for the wavelength dependence of the sensitivity of the detectors and throughput of the monochromators. The **Nap**/**CzPhONI** composite as well as the **Nap** neat thin film samples were spin-coated from their corresponding chloroform solutions with concentration of 10 mg/mL at a speed of 1500 rpm/min on quartz substrates for 40 s. Cyclic voltammetry measurements were performed in anhydrous acetonitrile (5×10^{-4} mol L^{-1}) solutions of **Nap1**~**3**, using 0.10 mol L^{-1} Bu_4NClO_4 as the supporting electrolyte under N_2 atmosphere on a LK 2010A electrochemical work station at room temperature, and the three-electrode cell comprised a Pt working electrode, a Pt wire counter electrode, and a $Ag/AgNO_3$ (0.1 M in acetonitrile) reference electrode. A ferrocene/ferrocenium redox couple was employed as the external standard.

2.2 OLED fabrication and measurements

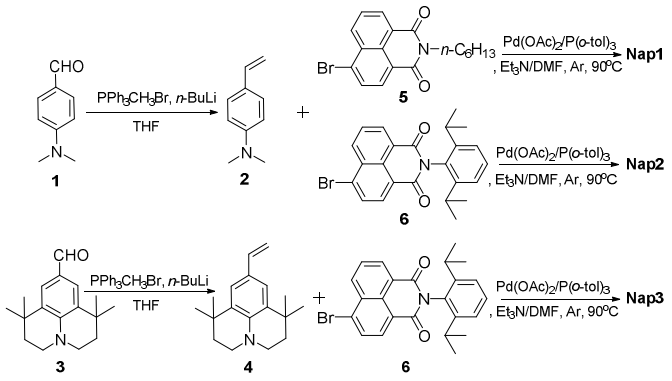

Scheme 1 Synthetic routes to the objective compounds.

Indium–tin oxide (ITO) coated glass substrate was cleaned by sonication successively in alcohol, acetone, methanol, and deionized water, followed by UV-ozone oxygen plasma treatment for 2 min before use. Organic functional layers were thermo-evaporated in vacuum (3×10^{-4} Pa) with a deposition rate of 0.1 nm s^{-1}. After deposition of the organic layers, the LiF-Al cathode was prepared first by thermal deposition of a LiF thin film (1 nm) followed by the deposition of an Al layer (80 nm). The active area of the OLEDs was 1×1 mm^2. The thicknesses of the organic layers and the cathode were controlled using a quartz crystal thickness monitor. The luminance-voltage-current density (*L-V-J*) characteristics of the OLEDs were measured with a Keithley 2611 Source Meter and a PR705 Spectra Colorimeter, which can also record EL spectra and CIE coordinates accurately. All the measurements on the devices were carried out in ambient atmosphere without further encapsulation.

2.3 Synthesis

The synthetic routes to **Nap1~3** are outlined in Scheme 1. Intermediates **2**,[25] **3**,[26] **5**,[27] **6**[28] were synthesised according to literature reports.

1,1,7,7-Tetramethyl-9-vinyl-2,3,6,7-tetrahydro-1*H*,5*H*-pyrido[3,2,1-*ij*]quinolone (4) *n*-Butyl lithium (1.0 mL of 2.5 mol L^{-1} *n*-hexane solution) was added dropwise to a suspension of PPh_3CH_3Br (0.90 g, 2.3 mmol) in anhydrous degassed THF (10.0 mL). The yellow solution was allowed to stir for 30 min, then a solution of **3** (0.4 g, 1.6 mmol) in 5.0 mL anhydrous degassed THF was added. After being stirred for 20 min, the yellow suspension was poured into saturated aqueous ammonium chloride, and then extracted by petroleum ether (4 × 15 mL). The organic layer was dried over anhydrous Na_2SO_4, and concentrated in vacuum. The resulting crude product was purified by silica gel column chromatography (eluent: petroleum ether/ethyl acetate=20/1, v/v) to give **4** as a yellowish liquid (0.3 g, 50%). δ_H (400 MHz; $CDCl_3$; Me_4Si) 7.07 (2H, s, ArH), 6.62 (1H, dd, J_1 = 17.2 Hz, J_2 = 10.8 Hz, =CH), 5.51 (1H, dd, J_1 = 17.6 Hz, J_2 = 1.6 Hz, =CH), 4.99 (d, J_1 = 10.0 Hz, J_2 = 1.6 Hz, 1H, =CH), 3.18 (t, *J* = 6.0 Hz, 6H, -NCH_2), 1.45 (t, *J* = 6.0Hz, 1H, Ar-CH_2), 1.30 (s, 12H, -CH_3).

(*E*)-6-(4-(dimethylamino)styryl)-2-hexyl-1*H*-benzo[*de*] isoquinoline-1,3(2*H*)-dione (Nap1). A schlenk flask was charged with a mixture of **2** (0.13 g, 0.9 mmol), **5** (0.30 g, 0.9 mmol), $Pd(OAc)_2$ (3.5 mg, 0.02 mmol), P(*o*-tolyl)$_3$ (8.3 mg, 0.03 mmol), triethylamine (6.0 mL) and *N*,*N*-dimethylformamide (DMF) (7.0 mL). The reaction mixture was heated at 90 °C for 24 h under argon. After being cooled to room temperature, the mixture was poured into water (100 mL), extracted by dichloromethane (4 × 20 mL), and the organic phase was combined and washed by brine, then dried over anhydrous Na_2SO_4. After the solvent was removed under vacuum, the crude product was purified by column chromatography over silica gel (eluent: petroleum ether/dichloromethane=15/1, v/v), followed by recrystallization from a mixture of cyclohexane and dichloromethane to afford pure **Nap1** as a red solid (0.1 g, 30%). δ_H (400 MHz; DMSO-d_6; Me_4Si) 9.00 (1H, d, *J* = 9.2 Hz, ArH), 8.53 (1H, d, *J* = 7.2 Hz, ArH), 8.45 (1H, d, *J* = 8.0 Hz, ArH), 8.21 (1H, d, *J* = 8.4 Hz, ArH), 7.96 (1H, d, *J* = 16.0 Hz, =CH), 7.89 (1H, t, J_1 = 7.6 Hz, J_2 = 8.0 Hz, ArH), 7.71 (2H, d, *J* = 8.4 Hz, ArH), 7.55 (1H, d, *J* =16.0 Hz, =CH), 6.89 (2H, d, *J* = 8.4 Hz, ArH), 4.05 (2H, t, *J* = 7.2 Hz, -NCH_2), 3.00 (6H, s, -NMe_2), 1.64 (m, 2H, -CH_2, -CH_3), 1.31 (m, 6H, -CH_2), 0.87 (m, 3H, -CH_3). δ_C (100 MHz; $CDCl_3$; Me_4Si) 164.4, 164.2, 150.9, 142.4, 135.6, 131.2, 131.0, 130.1, 129.4, 128.9, 128.5, 126.3, 124.8, 123.1, 122.9, 118.4, 112.2, 40.5, 40.3, 31.6, 28.1, 26.8, 22.6, 14.1. FT-IR ν_{max}/cm^{-1} 1655(C=O), 1358(C-N). HRMS $(ESI)^+$ *m/z*: calcd. for $[M + H]^+$: $C_{28}H_{31}N_2O_2^+$, 427.2380; found, 427.2365.

(*E*)-2-(2,6-di(isopropyl)phenyl)-6-(4-(dimethylamino)styryl) -1*H*-benzo[*de*]isoquinoline-1,3(2*H*)-dione (Nap2). Compound **Nap2** was prepared as a red solid with a yield of 50% using the similar procedure for the synthesis of **Nap1**, but with **5** rather than **6** as the reactant. δ_H (400 MHz; DMSO-d_6; Me_4Si) 9.11 (1H, d, *J* = 8.8 Hz, ArH), 8.59 (1H, d, *J* = 6.8 Hz, ArH), 8.50 (1H, d, *J* = 8.0 Hz, ArH), 8.25 (1H, d, *J* = 8.0 Hz, ArH), 8.01 (1H, d, *J* = 16.0 Hz, =CH), 7.93 (1H, t, J_1 = 6.4 Hz, J_2 = 8.0 Hz, ArH), 7.73 (2H, d, *J* = 8.8 Hz, ArH), 7.60 (1H, d, *J* =15.6 Hz, =CH), 7.45 (1H, t, *J* = 7.6 Hz, ArH), 7.33 (2H, d, *J* = 7.6 Hz, ArH), 6.78 (2H, d, *J* = 8.8 Hz, ArH), 3.00 (6H, s, -NMe_2), 2.66 (2H, m, Ar-CH) 1.05 (12H, d, *J* =6.8 Hz, -CH_3). δ_C (100 MHz; $CDCl_3$; Me_4Si) 164.4, 164.2, 145.7, 142.8, 135.9, 131.7, 131.6, 131.1, 130.4, 129.6, 129.6, 129.4, 128.6, 126.4, 124.0, 123.1, 123.0, 120.4, 118.4, 112.4, 40.4, 29.1, 24.0, 8.1. FT-IR ν_{max}/cm^{-1} 1661(C=O), 1352(C-N). HRMS $(ESI)^+$ *m/z*: calcd. for $[M + H]^+$: $C_{34}H_{35}N_2O_2^+$, 503.2693; found, 503.2676.

(*E*)-2-(2,6-di(isopropyl)phenyl)-6-(2-(1,1,7,7-tetramethyl-2,3,6,7-tetrahydro-1*H*,5*H*-pyrido[3,2,1-*ij*]quinolin-9-yl) vinyl)-1*H*-benzo[*de*]isoquinoline-1,3(2*H*)-dione (Nap3). Compound **Nap3** was prepared as a dark red solid with a yield of 24% using the similar procedure for the synthesis of **Nap1**, but with **4** and **6** rather than **2** and **5** as the reactants. The crude product was purified by column chromatography over silica gel (eluent: petroleum ether/dichloromethane = 15/1, v/v), followed by recrystallization from a mixture of *n*-hexane and dichloromethane for three times. δ_H (400 MHz; DMSO-d_6; Me_4Si) 9.16 (1H, d, *J* = 8.4 Hz, ArH), 8.60 (1H, d, *J* = 7.2 Hz,

Table 1 Photophysical data of the three objective molecules in solvents with different polarities (1.0×10^{-5} mol L^{-1}).

Solvent	NIM[a]			Nap1			Nap2			Nap3		
	λ_{absmax} (nm)	λ_{PLmax} (nm)	Φ_{PL}	λ_{absmax} (nm)	λ_{PLmax} (nm)	Φ_{PL}	λ_{absmax} (nm)	λ_{PLmax} (nm)	Φ_{PL}	λ_{absmax} (nm)	λ_{PLmax} (nm)	Φ_{PL}
CHX	-	-	-	440	514	0.22	447	517	0.16	479	553	0.24
CCl_4	-	-	-	450	543	0.29	457	546	0.28	488	567	0.42
Tol	448	552	0.81	461	580	0.42	468	585	0.42	505	622	0.24
$CHCl_3$	461	624	0.36	471	634	0.62	479	637	0.64	511	680	0.45
THF	450	607	0.54	466	655	0.59	473	658	0.54	510	696	0.29
CH_2Cl_2	-	-	-	470	669	0.51	477	672	0.50	519	722	0.09
Acetone	448	658	0.06	464	698	0.08	471	702	0.08	510	750	0.00

[a] Photophysical data derived from reference 24; λ_{absmax} : absorption maximum; λ_{PLmax} : PL emission maximum; Φ_{PL}: absolute PL quantum yield.

ArH), 8.49 (1H, d, J = 8.0 Hz, ArH), 8.25 (1H, d, J = 8.0 Hz, ArH), 7.95 (2H, m, ArH, =CH), 7.57 (1H, d, J = 16.0 Hz, =CH), 7.52 (2H, s, ArH), 7.45 (1H, t, J_1 = 7.6 Hz, ArH), 7.34 (2H, d, J = 7.6 Hz, ArH), 3.23 (4H, t, J_1 = 6.4 Hz, J_2 = 6.0 Hz, -NCH_2), 2.67 (2H, m, Ar-CH), 1.73 (4H, t, J_1 = 5.6 Hz, J_2 = 6.0 Hz, Ar-CH_2), 1.32 (12H, s, -CH_3), 1.06 (12H, d, J = 4.0 Hz, -CH_3). δ_C (100 MHz; $CDCl_3$; Me_4Si) 164.5, 164.2, 145.7, 143.2, 137.0, 131.8, 131.6, 131.1, 130.5, 129.6, 129.4, 126.3, 123.9, 123.3, 123.1, 122.8, 119.9, 117.0, 46.8, 36.4, 32.3, 30.8, 29.1, 24.0. FT-IR ν_{max}/cm^{-1} 1661 (C=O), 1576 (C-N). HRMS $(ESI)^+$ m/z: calcd. for $[M + H]^+$: $C_{42}H_{47}N_2O_2^+$, 611.3632; found, 611.3618.

3. Results and discussion

3.1 Photophysical properties in dilute solutions

The UV-Vis absorption spectra of **Nap1**~**3** in dilute solutions with different polarities are illustrated in Figure 2, and the corresponding data are summarized in Table 1. In similar solvent, the absorption maximum (λ_{absmax}) of **Nap2** is slightly red-shifted (~ 7 nm) compared with that of **Nap1**; but the λ_{absmax} of **Nap3** is considerably red-shifted (> 30 nm) than those of **Nap1** and **Nap2**. Therefore, the replacement of the *n*-hexyl bonding to the imide nitrogen atom into a 2,6-di(isopropyl) phenyl group would just bring a little effect on the conjugation length of these compounds; but the presence of a TMJ rather than a DMAP donor subunit in **Nap3** would endow it with much extended π-conjugation system. As expected, in every solvent, the absorption bands of all the three objective compounds are red-shifted than that of **NIM**,[24] confirming that the bandgaps of **Nap1**~**3** are narrower than that of **NIM**, which should be chiefly attributed to the more electron-donating capability of DMAP and TMJ groups than that of DPAP. With an increase in solvent polarity from cyclohexane (CHX) to dichloromethane (DCM), the absorption bands of **Nap1**~**3** show 20~30 nm red-shifts, indicative of the ICT character of the three compounds in their ground states.[20,29]

Consistent with the absorption characteristics of **NIM** and **Nap1**~**3**, the PL emission maximum (λ_{PLmax}) of **Nap3** is more bathochromic-shifted (~ 30 nm) than that of **Nap2** or **Nap1** in every solvent; the λ_{PLmax} of **Nap2** is just slightly (3~5 nm) red-shifted than that of **Nap1**; and the λ_{PLmax}s of **Nap1**~**3** are significantly red-shifted than that of **NIM** (Figure 3 and Table 1). In comparison with their absorption spectra, the fluorescent spectra of **Nap1**~**3** were observed to show more significant positive solvatochromism (e.g., for **Nap3**: λ_{PLmax} = 553 nm in CHX; λ_{PLmax} = 622 nm in toluene; λ_{PLmax} = 680 nm in

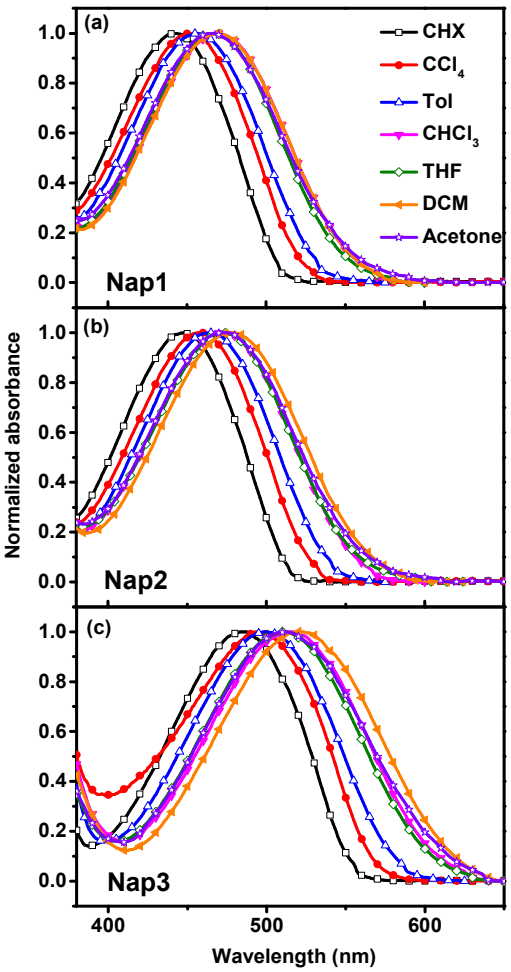

Figure 2 Normalized absorption spectra of the three objective compounds in solvents with different polarities. (a) **Nap1**; (b) **Nap2**; and (c) **Nap3**.

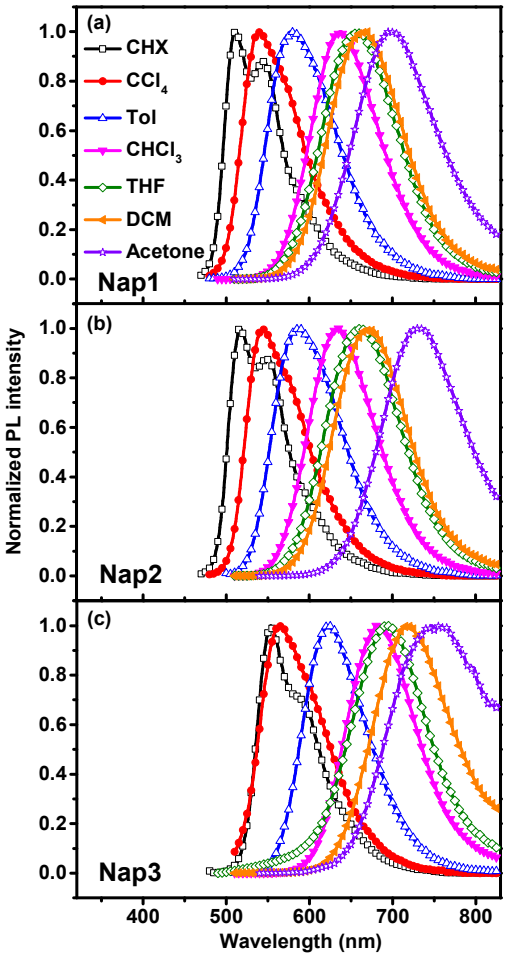

Figure 3 Normalized PL emission spectra of the three objective compounds in solvents with different polarities. (a) **Nap1**; (b) **Nap2**; and (c) **Nap3**.

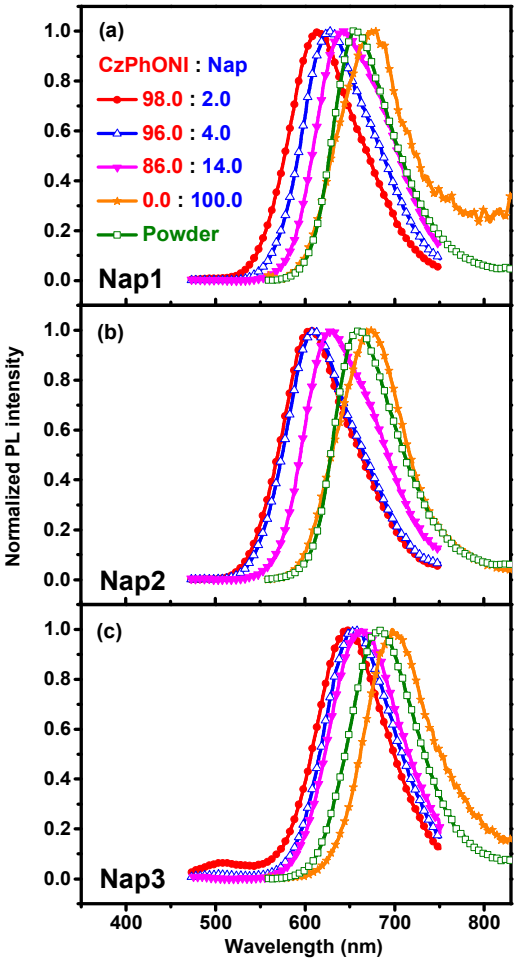

Figure 4 Normalized PL emission spectra of the **Nap/CzPhONI** blend films (λ_{ex} = 390 nm) and the crystalline powder samples as well as the neat film samples of **Nap**s (λ_{ex} = 490 nm). (a) **Nap1**; (b) **Nap2;** and (c) **Nap3**.

chloroform; λ_{PLmax} = 722 nm in DCM; and λ_{PLmax} = 750 nm in acetone), indicative of the strong ICT character of the lowest singlet excited states of **Nap1**~**3**. This deduction was further confirmed by the Lippert-Mataga plots of **Nap1**~**3** (see Figure S1, ESI), since good linear correlations between solvent polarity parameter and Stokes shifts could be achieved in all these **Nap**s. It should be pointed out that in solvents with moderate polarity like chloroform and tetrahydrofuran (THF), **Nap1**~**3** could emit red fluorescence with high PL quantum yields (PLQY, Φ_{PL}). For example, in THF solution, both **Nap1** and **Nap2** show λ_{PLmax}s of > 650 nm and Φ_{PL}s of > 0.5; and the chloroform solution of **Nap3** displays a λ_{PLmax} of 680 nm and a Φ_{PL} of 0.45. With further increased solvent polarity to acetone, the PL emission spectra of **Nap1**~**3** were all observed to shift to near infrared region approaching ~ 750 nm; but their Φ_{PL}s were found to decrease drastically, which might arise from the much intensified non-radiative internal conversion processes in these compounds due to their much lowered energy gaps.[9] Nevertheless, taking into consideration that **Nap1**~**3** could emit highly efficient red fluorescence in solvents with medium polarity, they might act as promising red EL materials.

3.2 PL emission properties in crystalline powder and thin film states

To investigate their potentials as red light-emitting materials in OLEDs, PL emission spectra of **Nap1**~**3** in crystalline powder and thin film states were recorded. As shown in Figure 4 and Table 2, in both powder and film states, all the three compounds could emit standard-red fluorescence with λ_{PLmax} of 660~700 nm, and **Nap3** shows the most red-shifted emission band. In each case, the PL spectrum of the film sample of **Nap** is slightly broader and red-shifted than that of the crystalline powder sample, which should be attributed to their different molecular conformations in crystalline and amorphous states.[30]

Despite the fact that in dilute solutions, the fluorescence band of **Nap2** is slightly red-shifted than that of **Nap1**, its λ_{PLmax} was observed to be even 6 nm blue-shifted than that of **Nap1** in neat film state (669 nm *vs* 675 nm), and its Φ_{PL} is also higher than that of **Nap1** (0.02 *vs* 0.01). Hence we could infer that the presence of a more bulky 2,6-di(isopropyl)phenyl rather than a *n*-hexyl group in **Nap2** should be propitious to the suppression of intermolecular interactions of these fluorophores, and hence

Table 2 Fluorescence data and PLQYs of **Nap**/**CzPhONI** blend films, neat films and crystalline powders of the three objective molecules.

Doping ratio (wt%)	Nap1		Nap2		Nap3	
	λ_{PLmax}[a] (nm)	Φ_{PL}[a]	λ_{PLmax}[a] (nm)	Φ_{PL}[a]	λ_{PLmax}[a] (nm)	Φ_{PL}[a]
2	613	0.37	608	0.46	646	0.23
4	622	0.29	612	0.38	655	0.21
14	641	0.16	632	0.27	663	0.15
Neat film	678	0.01	673	0.02	703	0.01
Powder	659	0.01	659	0.04	680	0.02

[a] λ_{ex} = 390 nm for the blend films; λ_{ex} = 490 nm for the neat films and crystalline powders.

could promote less concentration quenching. Although the Φ_{PL}s of these neat film samples are rather low (≤ 0.02), which would limit their potentials as high-performance non-doped red EL luminogens, the relatively high Φ_{PL}s of **Nap1**~**3** in medium-polarity solvents spur us to prepare guest/host composite films using **Nap1**~**3** as dopants. As the compound **CzPhONI** (structure shown in Figure 5) we have developed recently is a high performance host material for an orange naphthalimide guest compound,[23] herein we chose it as the host material to fabricate **Nap**/**CzPhONI** guest/host composite films with different doping-levels.

As shown in Figure 4 and Table 2, for all the three compounds, with increasing concentration of **Nap** from 2 wt% to 14 wt%, the λ_{PLmax} of the corresponding **Nap**/**CzPhONI** composite film red-shifts gradually. Excitingly, at a relatively high doping-level of 14 wt%, the film samples with **Nap1** and **Nap2** as guests could emit red fluorescence with λ_{PLmax} of 630~640 nm; and the 14 wt% **Nap3** composite film could emit standard-red fluorescence with satisfactory chromaticity (λ_{PLmax} = 663 nm). Analogous to the PL emission property of their neat films, in every doping-level, the λ_{PLmax} of **Nap2** was observed to be blue-shifted for 5~10 nm than that of **Nap1**, validating the more suppressed intermolecular interactions in **Nap2** than **Nap1**. In composite films with **Nap1** and **Nap2** as guests, no emission from the **CzPhONI** host (λ_{PLmax} ~500 nm)[23] could be discerned at each doping-level, indicative of the efficient energy transfer between the host and guest compounds. While for **CzPhONI**/**Nap3** composite films, the emission band from **CzPhONI** is discernible at relative low doping-level of 2 wt%, hence the energy transfer efficiency between **CzPhONI** and **Nap3** should not be as high as that between **CzPhONI** and **Nap1**/**Nap2**.

In comparison with those of the neat films, the Φ_{PL}s of the guest/host blend film samples are much improved (Table 2). For all the three compounds, the highest PLQYs of the blend films are obtained at the lowest doping-level of 2 wt%. With increasing guest doping ratios from 2 wt% to 14 wt%, the Φ_{PL} of **Nap1**-based film drops considerably from 0.37 to 0.16; while the Φ_{PL}s of **Nap2**- and **Nap3**-based samples are lowered from 0.46 to 0.27 and from 0.23 to 0.15, respectively, both are less significant than that of the **Nap1**-based one, indicating that **Nap2** and **Nap3** show more alleviated self-quenching relative to **Nap1**. Consequently, owing to the concurrent presence of a strong electron-donating TMJ group and a bulky 2,6-di(isopropyl)phenyl substituent, **Nap3** possesses not only an extended π-conjugation system, but also alleviated concentration quenching, hence is a perspective candidate as standard-red EL material.

3.3 Electrochemical properties

To estimate the energy levels of the frontier orbitals of **Nap1**~**3**, their electrochemical property were investigated by cyclic voltammetry (CV) in degassed 5 × 10^{-4} mol L^{-1} anhydrous acetonitrile solutions with Fc/Fc^+ redox couple as the external standard, and the cyclic voltammograms are shown in Figure S2 (in ESI). During the anodic scan from 0 V to 0.50 V, both **Nap1** and **Nap2** show reversible oxidation waves with half wave potentials ($E_{1/2}$) of 0.24 V *vs* Fc/Fc^+; but **Nap3** shows a reversible oxidation wave with $E_{1/2}$ of 0.05 V *vs* Fc/Fc^+. Upon cathodic scan from 0 V to –1.95 V, **Nap1** shows a reversible reduction wave with $E_{1/2}$ of -1.70 V *vs* Fc/Fc^+; while both **Nap2** and **Nap3** show reversible reduction waves with $E_{1/2}$ of -1.66 V *vs* Fc/Fc^+. Hence the calculated electrochemical band-gaps of **Nap1**~**3** are 1.94 eV, 1.90 eV and 1.71 eV in sequence, which are consistent with their optical bandgaps (2.19 eV, 2.17 eV and 1.85 eV for **Nap1**~**3** in sequence) deduced from the onset of their UV-Vis absorption spectra in dilute acetonitrile solutions (Figure S3 in ESI).

In comparison with the Fc/Fc^+ redox couple whose energy level is −4.88 eV in vacuum,[31] the HOMO energy levels of **Nap1**~**3** are calculated to be –5.12 eV, –5.12 eV and –4.93 eV in turn; and their LUMO energy levels are calculated to be –3.18 eV, –3.22 eV and –3.22 eV in sequence. As the HOMO and LUMO energy levels of **CzPhONI** are –5.60 eV and –3.10 eV, respectively,[23] the HOMO energy difference between **CzPhONI** and **Nap1**~**2** is 0.48 eV, but that between the HOMOs of **CzPhONI** and **Nap3** is as large as 0.67 eV. Hence **CzPhONI** should be a more ideal host material for **Nap1**~**2** than **Nap3**, which may account for the more efficient energy transfer process between **CzPhONI** and **Nap1**~**2** than **Nap3**.

3.4 Electroluminescent properties

Based on these photophysical and electrochemical experimental results, thermo-evaporated OLEDs with **Nap3**/**CzPhONI** composite film as light-emitting layer (EML) were fabricated. The device structure is ITO/MoO_3 (1 nm)/TcTa (40 nm)/**CzPhONI**:**Nap3** (x wt%) (20 nm)/TPBI (45 nm)/LiF (1nm)/Al (80 nm), where TcTa (4,4',4''-tri(*N*-carbazolyl) triphenylamine) serves as the hole-transporting material (HTM), TPBI (1,3,5-tris(1-phenyl-1*H*-benzo[*d*]imidazol-2-yl)benzene) serves as the electron-transporting material (ETM). The energy level diagram of the devices is shown in Figure 5. According to the PL characterization results, device **I**, **II** and **III** with **Nap3** concentration of 2 wt%, 4 wt% and 14 wt% respectively were prepared. The EL spectra and the luminance-voltage-current density (*L*-*V*-*J*) characteristics of devices **I**~**III** are shown in Figure 6, and some representative EL performance data are summarized in Table 3.

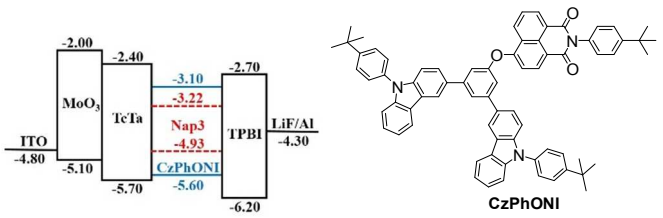

Figure 5 Device configuration and energy band diagram of devices **I**, **II**, and **III** (left); and molecular structure of the host compound **CzPhONI** (right).

Devices **I**~**III** all display bias-independent EL spectra, with λ_{ELmax} of 636 nm, 644 nm and 657 nm (vide Figure 6a and Figure S4 in ESI), and CIE coordinates of (0.62, 0.37), (0.65,0.34) and (0.67, 0.32) in sequence. Hence devices **I** and **II** can emit red EL, but device **III** shows standard-red EL with satisfactory chromaticity. Compared with the corresponding PL spectra of their EML, the EL spectra of all the devices are much broadened and slightly blue-shifted. Because the emission band of **Nap3** correlates highly with environment polarity, and the EML of the OLEDs is as thin as 20 nm, carrier recombination may occur not only within the EML, but also at the TcTa/EML or EML/TPBI interfaces, these may account for the broadened and blue-shifted EL spectra of these devices. In addition, although the emission from **CzPhONI** is discernible in the PL spectrum of 2 wt% **Nap3**/**CzPhONI** composite film, it could not be observed in the EL spectrum of device **I**, indicative of the more efficient energy transfer and/or charge carrier trapping on **Nap3** in the EL process. As shown in Figure 6b, under similar driving voltages, the current density of device **II** is lower than that of device **I**; but that of the more heavily-doped device **III** is comparable with that of device **I**. Consequently, it should be the energy transfer mechanism that dominates the EL emission process in device **I** and **II** whose guest doping-levels are relatively low; but it should be the direct charge carrier trapping mechanism that governs the EL process in device **III**.[32] In fact, according to the energy level diagram of the devices (Figure 5), **Nap3** should act as efficient hole-carrier traps due to its much higher HOMO energy level than those of the host and HTM.

All the three devices display comparable turn-on voltages of 3.1 V. Device **I** exhibits relative high EL performance with L_{max}, CE_{max} and EQE_{max} of 10900 cd m^{-2}, 1.9 cd A^{-1} and 2.1%, respectively, indicating that **Nap3** is a quite promising guest compound for OLED applications. However, the chromaticity of this device is still unsatisfactory. With increasing doping-level to 4 wt%, the resulting device **II** shows EL that approaches standard-red emission, with L_{max}, CE_{max} and EQE_{max} of 6600 cd m^{-2}, 1.1 cd A^{-1} and 1.8%, respectively. For device **III** with further increased doping-level, it could emit standard-red EL with L_{max} of 2660 cd m^{-2}, CE_{max} of 0.7 cd A^{-1}, and EQE_{max} of 1.8%. It should be pointed out that compared with the state-of-art standard-red electrofluorescent OLEDs, the PLQYs of the active layers using **Nap3** as guest dopant are unsatisfactory, which may eventually limit the efficiency of the devices. Nevertheless, as the dilute chloroform solution of **Nap3** could emit standard-red fluorescence with Φ_{PL} of ~ 0.45,

Table3 EL characteristics of the devices using **Nap3** as guest dopant

Device	V_{on} (V)	L_{max} (cd m^{-2})	EQE_{max} (%)	CE_{max} (cd A^{-1})	λ_{ELmax} (nm)	CIE (x, y)
I	3.1	10900	2.1	1.9	636	(0.62, 0.37)
II	3.1	6600	1.8	1.1	644	(0.65, 0.34)
III	3.1	2660	1.8	0.7	657	(0.67, 0.32)

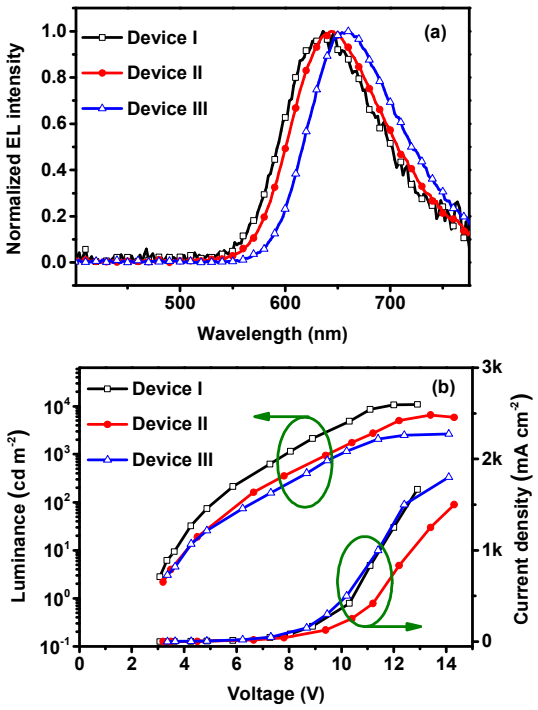

Figure 6 (a) EL spectra of the three devices (under driving current density of 0.5 mA cm^{-1}); (b) Luminance-voltage-current density characteristics of the devices.

the PLQY of the EML with **Nap3** as the guest compound might be enhanced drastically if more appreciate host material were used. Moreover, the device structure, doping level and layer thickness used here have not been optimized for either low driving voltage or high efficiency, thus much improved EL performance should be expected after further optimization has been carried out on these issues.

Conclusions

Using electron-rich arylamino groups as the donor constructive units, three red-emissive naphthalimide derivatives were designed and synthesized, and the correlations between the molecular structures and photophysical properties of these compounds have been investigated. The results indicated that the presence of a more electron-donating 1,1,7,7-tetramethyljulolidin-9-yl in these fluorophores would endow them with more red-shifted emission bands; while the presence of a bulky 2,6-di(isopropyl)phenyl group on the imide nitrogen atom of these luminogens would endow them with more alleviated intermolecular interactions. Consequently, the objective compound **Nap3** bearing both 1,1,7,7-tetramethyljulolidin-9-yl and 2,6-di(isopropyl)phenyl groups

not only shows standard-red fluorescence with satisfactory chromaticity, but also shows suppressed concentration quenching. Using **Nap3** as the guest dopant, a heavily-doped standard-red OLED was achieved, whose CIE coordinates, EQE_{max} and CE_{max} are (0.67, 0.32), 1.8% and 0.7 cd A^{-1}, respectively. To the best of our knowledge, this is the first example of standard-red-emissive 1,8-naphthalimide derivative for OLED applications. All these preliminary results indicated that through rational molecular design, 1,8-naphthalimide derivatives could act as quite promising standard-red light-emitting materials for OLED applications.

Acknowledgements

We acknowledge the financial support for this work by National Natural Science Foundation of China (Project Nos. 21372168, 21190031 and 21321061), and CAS Innovation Program. We are also grateful to the Comprehensive Training Platform of Specialized Laboratory, College of Chemistry, SCU and the Analytical and Testing center, SCU for providing NMR, FT-IR and HRMS data of the intermediates and objective compounds.

Notes and references

[a] Key Laboratory of Green Chemistry and Technology of Ministry of Education, College of Chemistry, Sichuan University, Chengdu, 610064, PR China;
[b] State Key Laboratory of Luminescence and Applications, Changchun Institute of Optics, Fine Mechanics and Physics, Chinese Academy of Sciences, Changchun 130033, PR China;
‡ These authors contributed equally.

† Electronic Supplementary Information (ESI) available: Lippert-Mataga plots of **Nap1~3**, cyclic voltammogram of **Nap1~3**, EL spectra of devices **I~III**, current efficiency-current density characteristics of devices **I~III**, ^{1}H NMR, ^{13}C NMR, FT-IR, and HRMS spectra of **Nap1~3**.
See DOI: 10.1039/b000000x/

1 For reviews, see : a) C. Fan, C. Yang, *Chem. Soc. Rev.*, 2014, **43**, 6439-6469; b) L. Bao, M. D. Heagy, *Current Org. Chem.*, 2014, **18**, 740-772; c) M. Zhu, C. Yang, *Chem. Soc. Rev.*, 2013, **42**, 4963-4976; d) C. Murawski, K. Leo, M. C. Gather, *Adv. Mater.*, 2013, **25**, 6801-6827; e) S. Schmidbauer, A. Hohenleutner, B. König, *Adv. Mater.*, 2013, **25**, 2114-2129; f) H. Sasabe, J. Kido, *J. Mater. Chem. C*, 2013, **1**, 1699-1707; g) Y. Chen, D. Ma, *J. Mater. Chem.*, 2012, **22**, 18718-18734.

2 a) A. Benor, S.-Y. Takizawa, C. Pérez-Bolívar, P. Anzenbacher, *Org. Electron.*, 2010, **11**, 938-945; b) J.-H. Jou, J.-R. Tseng, K.-Y. Tseng, W.-B. Wang, Y.-C. Jou, S.-M. Shen, Y.-L. Chen, W.-Y. Huang, S.-Z. Chen, T.-Y. Ding, H.-C. Wang, *Org. Electron.*, 2012, **13**, 2893-2897.

3 a) T. Peng, G. Li, Y. Liu, Y. Wu, K. Ye, D. Yao, Y. Yuan, Z. Hou, Y. Wang, *Org. Electron.*, 2011, **12**, 1068-1072; b) J. W. Sun, J.-H. Lee, C.-K. Moon, K.-H. Kim, H. Shin, J.-J. Kim, *Adv. Mater.*, 2014, **26**, 5684-5688.

4 J. Chen, D. Ma, *J. Luminesc.*, 2007, **122-123**, 636-638.

5 T. Arakane, M. Funahashi, H. Kuma, K. Fukuoka, K. Ikeda, H. Yamamoto, F. Moriwaki, C. Hosokawa, *SID Digest*, 2006, **37**, 37-40.

6 a) B.-J. Jung, J.-I. Lee, H. Y. Chu, L.-M. Do, J. Lee, H.-K. Shim, *J. Mater. Chem.*, 2005, **15**, 2470-2475; b) Y. Qiu, P. Wei, D. Zhang, J. Qiao,; L. Duan, Y. Li, Y. Gao, L. Wang, *Adv. Mater.*, 2006, **18**, 1607-1611; c) Z. Zhao, J. Geng, Z. Chang, S. Chen, C. Deng, T. Jiang, W. Qin, J. W. Y. Lam, H. S. Kwok, H. Qiu, B. Liu, B. Z. Tang, *J. Mater. Chem.*, 2012, **22**, 11018-11021; d) K. H. Lee, Y. K. Kim, S. S. Yoon, *J. Nanosci. Nanotechn.*, 2012, **12**, 4203-4206; e) W. Li, Y. Pan, R. Xiao, Q. Peng, S. Zhang, D. Ma, F. Li, F. Shen, Y. Wang, B. Yang, Y. Ma, *Adv. Funct. Mater.*, 2014, **24**, 1609-1614; f) W. Zhang, Z. He, Y. Wang, S. Zhao, *Thin Solid Films*, 2014, **562**, 299-306.

7 S. Forget, S. Chenais, D. Tondelier, B. Geffroy, I. Gozhyk, M. Lebental, E. Ishow, *J. Appl. Phys.*, 2010, **108**, 064509.

8 Y.-T. Lee, C.-L. Chiang, C.-T. Chen, *Chem. Commun.*, 2008, **44**, 217-219.

9 X. H. Zhang, B. J. Chen, X. Q. Lin, O. Y. Wong, C. S. Lee, H. L. Kwong, S. T. Lee, S. K. Wu, *Chem. Mater.*, 2001, **13**, 1565-1569.

10 C.-T. Chen, *Chem. Mater.*, 2004, **16**, 4389-4400.

11 a) B.-B. Jang, S. H. Lee, Z. H. Kafafi, *Chem. Mater.*, 2006, **18**, 449-457; b) X. H. Zhang, Z. Y. Xie, F. P. Wu, L. L. Zhou, O. Y. Wong, C. S. Lee, H. L. Kwong, S. T. Lee, S. K. Wu, *Chem. Phys. Lett.*, 2003, **382**, 561-566; c) C. A. Barker, X. Zeng, S. Bettington, A. S. Batsanov, M. R. Bryce, A. Beeby, *Chem.-Eur. J.*, 2007, **13**, 6710-6717.

12 a) J. L. Sessler, V. L. Capuano, A. Harriman, *J. Am. Chem. Soc.*, 1993, **115**, 4618-4628; b) P. D. Rao, S. Dhanalekshmi, B. J. Littler, J. S. Lindsey, *J. Org. Chem.*, 2000, **65**, 7323-7344.

13 a) X. Sun, Y. Liu, X. Xu, C. Yang, G. Yu, S. Chen, Z. Zhao, W. Qiu, Y. Li, D. Zhu, *J. Phys. Chem. B*, 2005, **109**, 10786-10792; b) Y. Li, G. Zhang, G. Yang, Y. Guo, C. Di, X. Chen, Z. Liu, H. Liu, Z. Xu, W. Xu, H. Fu, D. Zhang, *J. Org. Chem.*, 2013, **78**, 2926-2934; c) J.-Y. Yoon, J. S. Lee, S. S. Yoon, Y. W. Kim, *Bull. Korean Chem. Soc.*, 2014, **35**, 1670-1674.

14 a) W.-C. Wu, H.-C. Yeh, L.-H. Chan, C.-T. Chen, *Adv. Mater.*, 2002, **14**, 1072-1075; b) Y.-S. Lee, Z. Lin, Y.-Y. Chen, C.-Y. Liu, T. J. Chow, *Org. Electron.*, 2010, **11**, 604-612.

15 a) X. Sun, X. Xu, W. Qiu, G. Yu, H. Zhang, X. Gao, S. Chen, Y. Song, Y. Liu, *J. Mater. Chem.*, 2008, **18**, 2709-2715; b) B. R. Lee, W. Lee, T. L. Nguyen, J. S. Park, J.-S. Kim, J. Y. Kim, H. Y. Woo, M. H. Song, *ACS Appl. Mater. Interfaces*, 2013, **5**, 5690-5695; c) T. Khanasa, N. Prachumrak, R. Rattanawan, S. Jungsuttiwong, T. Keawin, T. Sudyoadsuk, T. Tuntulani, V. Promarak, *Chem. Commun.*, 2013, **49**, 3401-3403.

16 W. Zhang, Z. He, L. Mu, Y. Zou, Y. Wang, S. Zhao, *Dyes Pigm.*, 2010, **85**, 86-92.

17 a) C. W. Tang, S. A.VanSlyke, C. H. Chen, *J. Appl. Phys.*, 1989, **65**, 3610-3616; b) C. H. Chen, C. W. Tang, J. Shi, K. P. Klubek, *Macromol. Symp.*, 1997, **125**, 49-58; c) B.-J. Jung, C.-B. Yoon, H.-K. Shim, L.-M. Do, T. Zyung, *Adv. Funct. Mater.*, 2001, **11**, 430-434; d) E. J. Na, K. H. Lee, H. Han, Y. K. Kim, S. S. Yoon, *J. Nanosci. Nanotechnol.*, 2013, **13**, 554-557.

18 J. Liu, G. Tu, Q. Zhou, Y. Cheng, Y. Geng, L. Wang, D. Ma, X. Jing, F. Wang, *J. Mater. Chem.*, 2006, **16**, 1431-1438.

19 J. Liu, Y. Wang, G. Lei, J. Peng, Y. Huang, Y. Cao, M. Xie, X. Pu, Z. Lu, *J. Mater. Chem*, 2009, **19**, 7753-7758.
20 P. Wang, Z. Xie, S. Tong, O. Wong, C.-S. Lee, N. Wong, L. Hung, S. Lee, *Chem. Mater.*, 2003, **15**, 1913-1917.
21 J.-A. Gan, Q. L. Song, X. Y. Hou, K. C. Chen, H. Tian, *J. Photochem. Photobio. A : Chem.*, 2004, **162**, 399-406.
22 A. Islam, C.-C. Cheng, S.-H. Chi, S. J. Lee, P. G. Hela, I.-C. Chen, C.-H. Cheng, *J. Phys. Chem. B*, 2005,**109**, 5509-5517.
23 J. Zhou, P. Chen, X. Wang, Y. Wang, Y. Wang, F. Li, M. Yang, Y. Huang, J. Yu , Z. Lu, *Chem. Commun.*, 2014, **50**, 7586-7589.
24 H.-H. Lin, Y.-C. Chan, J.-W. Chen, C.-C. Chang, *J. Mater. Chem.*, 2011, **21**, 3170-3177.
25 C. A. Faler, M. M. Joullié, *Org. Lett.*, 2007, **9**, 1987-1990.
26 a) C.-T. Lee, A. T. Hu, *Dyes Pig.*, 2003, **59**, 63-69; b) B. Balaganesan, S.-W. Wen, C. H. Chen, *Tetrahedron Lett.*, 2003, **44**, 145-147; c) X. Jiang, X. Yang, C. Zhao, K. Jin, L. Sun, *J. Phys. Chem. C*, 2007, **111**, 9595-9602.
27 F. Yu, Y. Wang, W. Zhu, Y. Huang, M. Yang, H. Ai, Z. Lu, *RSC Adv.*, 2014, **4**, 36849-36853.
28 H. Marom, Y. Popowski, S. Antonov, M. Gozin, *Org. Lett.*, 2011, **13**, 5532-5535.
29 M. Ghasemian, A. Kakanejadifard, F. Azarbani, A. Zabardasti, S. Shirali, Z. Saki, S. Kakanejadifard, *Spectrochim. Acta, Part A*, 2015, **138**, 643-647.
30 C. Y. K. Chan, Z. Zhao, J. W. Y. Lam, J. Liu, S. Chen, P. Lu, F. Mahtab, X. Chen, H. H. Y. Sung, H. S. Kwok, Y. Ma, I. D. Williams, K. S. Wong, B. Z. Tang, *Adv. Funct. Mater.*, 2012, 22, 378-389.
31 a) X. Liu, B. B. Y. Hsu, Y. Sun, C.-K. Mai, A. J. Heeger, G. C. Bazan, *J. Am. Chem. Soc.*, 2014, **136**, 16144−16147; b) X. Liu, Y. Sun, B. B. Y. Hsu, A. Lorbach, L. Qi, A. J. Heeger, G. C. Bazan, *J. Am. Chem. Soc.*, 2014, **136**, 5697−5708.
32 a) M. A. Wolak, B.-B. Jang, L. C. Palilis, Z. H. Kafafi, *J. Phys. Chem. B*, 2004, **108**, 5492-5499; b) M. A. Wolak, J. Delcamp, C. A. Landis, P. A. Lane, J. Anthony, Z. Kafafi, *Adv. Funct. Mater.*, 2006, **16**, 1943-1949; c) K. H. Lee, M. H. Park, C. S. Kim, Y. K. Kim, S. S. Yoon, *Thin Solid Films*, 2011, **520**, 510-514.

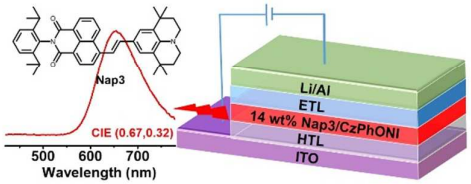

A 1,8-naphthalimide derivative has been demonstrated to be a high performance standard-red EL material.